PRAMANA
— journal of
physics

Vol. 82, No. 2
February 2014
pp. 321–325

Picosecond nonlinear optical properties of cuprous oxide with different nano-morphologies

P HARSHAVARDHAN REDDY, H SEKHAR and D NARAYANA RAO*
Laser Laboratory, School of Physics, University of Hyderabad, Hyderabad 500 046, India
*Corresponding author. E-mail: dnr.laserlab@gmail.com; dnrsp@uohyd.ernet.in

DOI: 10.1007/s12043-014-0684-y; ***e*Publication:** 8 February 2014

Abstract. Cuprous oxide nanoclusters, microcubes and microparticles were successfully synthesized by a simple co-precipitation method. Phase purity and crystallinity of the samples were studied by using X-ray powder diffraction. Transmission electron microscopy (TEM) images show different morphologies like nanoclusters, microcubes and microparticles. For linear and nonlinear optical measurements, the as-synthesized Cu_2O with different morphologies were dispersed in isopropanol solution. The absorption spectrum recorded in the visible regions shows peaks that depend on the morphology of the particles and the peak shifts towards red region as one goes from nanoclusters to microparticles. Simple open-aperture Z-scan technique is used to measure nonlinear optical properties of cuprous oxide at 532 nm, 30 ps excitation at 10 Hz repetition rate. Cuprous oxide nanoclusters show reverse saturable absorption (RSA) behaviour, the microcubes and microparticles at a similar concentration exhibit saturable absorption (SA) type of behaviour at lower peak intensities and exhibit RSA within SA at higher peak intensities. The results show that the transition from SA to RSA can be ascribed to the two-photon absorption (TPA) process.

Keywords. Nonlinear absorption; saturable absorption; reverse saturable absorption; nanocrystalline materials; cuprous oxide.

PACS Nos 42.65.–k; 73.63.Bd; 71.20.Nr

1. Introduction

The past few years have witnessed an increasing trend toward the synthesis of micro and nanostructures of Cu_2O with well-controllable size and shapes. Cu_2O is cheap, less toxic and naturally abundant. It is also an important inorganic p-type semiconductor with a direct band gap of 2.17 eV and can be used in solar cells, electrode material for lithium ion batteries, dilute magnetic semiconductor (DMS) and bio and gas sensors. It is possible to tune the band gap and influence the physical, chemical and electronic properties of the semiconductors by simply changing particle size from nano to submicron scale and by doping with transition metal ions [1–3]. The properties at nanoscale

are quite different from that of their bulk counterparts making them good candidates for various important applications in the field of material research.

In brief, nanotechnology is one of the most active research areas which find useful applications in different fields of science. Intense research is also pursued to develop new nonlinear optical materials with high optical nonlinearities and fast response time [4–8]. To find the nonlinear optical parameters nonlinear absorption (NLA), we utilized the standard Z-scan technique, which is a simple single-beam nonlinear transmission experiment [4]. Nonlinear interaction of electromagnetic radiation with matter can show two types of nonlinear absorption behaviour: (1) fall in absorption with intensity (saturable absorption (SA)) and used for optical pulse compression, optical switching, etc. (2) increase in absorption with intensity called reverse saturable absorption (RSA), which can be induced in the material either by excited state absorption (ESA) or by a two (multi) photon absorption (TPA) process. As the RSA materials show stronger absorption with increasing intensity/fluence, these materials help in optical limiting studies, where the material exhibits linear transmittance at lower intensities/fluence and limits to a threshold transmittance at higher intensities/fluences. ESA and TPA are two important processes leading to RSA behaviour in metals, semiconductors and organic materials [4–8]. Under resonant and near-resonant excitations, ESA is the dominant mechanism, whereas under nonresonant excitation TPA dominates the NLA behaviour. Under certain excitation conditions, both ESA and TPA may be operative simultaneously leading to higher nonlinearities.

The present work is focussed on the linear and nonlinear absorption properties of Cu_2O with different morphologies using a picosecond laser excitation.

2. Results and discussion

Cu_2O with different morphologies were prepared by simple chemical co-precipitation method [3]. The sample codes of the Cu_2O powders obtained by varying the concentration of NaOH as 0.5, 0.75 and 1.5 M are referred to as Cu_2O-I, Cu_2O-II and Cu_2O-III, throughout this paper.

X-ray powder diffraction (XRD) patterns of the as-prepared powders were recorded with the help of Inel-C120 X-ray diffractometer Co-Kα radiation of wavelength 0.17889 nm. Figure 1 shows the XRD pattern of the as-synthesized Cu_2O powders, all the peaks match well with the standard JCPDF File No. 05-0667.

Linear optical absorption spectra of the as-prepared Cu_2O powders were recorded by dispersing them in iso-propanol by ultrasonication for 15 min by using JASCO UV–Vis absorption spectrophotometer and are shown in figure 2. From UV–Vis absorption spectra, the optical band gaps of Cu_2O-I, Cu_2O-II and Cu_2O-III are calculated as 2.6, 2.3 and 2.1 eV respectively. Cu_2O-I, Cu_2O-II optical band gaps shift toward higher energy compared to the bulk Cu_2O band gap at 2.1 eV. This can be ascribed to the quantum confinement effect. The observed spectrum matches well with the Cu_2O spectrum.

The morphology and the particle sizes of the as-prepared powder samples were measured with TECNAI G^2 FEI F12 model. TEM samples were prepared by placing a drop of isopropanol dispersed with Cu_2O powder on carbon-coated copper grid to determine the particle morphology and lattice imaging. Figure 3 shows a set of typical TEM images

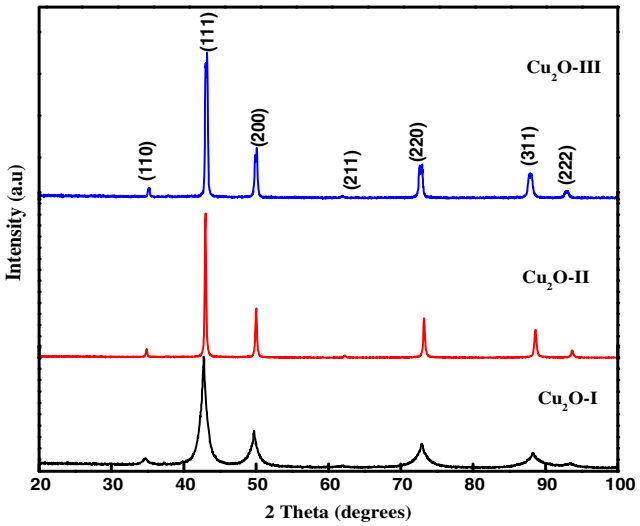

Figure 1. XRD pattern of the as-synthesized Cu_2O powders at different NaOH concentrations.

of Cu_2O powders. Cu_2O-I (figure 3a) particle size varied from 15 to 20 nm and agglomerated to 100–150 nm size. Cu_2O-II (figure 3b) powder morphology indicates that it is an aggregation of cubes with varying sizes from 100 to 150 nm. Cu_2O-III (figure 3) powders are of nearly micron size. OH^- ions affect the stability of Cu_2O with different morphologies [9]. High-resolution TEM images of Cu_2O nanoclusters and microcubes exhibit visible lattice fringes with interplanar spacing of 0.25 nm, corresponding to (1 1 1) reflection of the cubic crystal structure of Cu_2O.

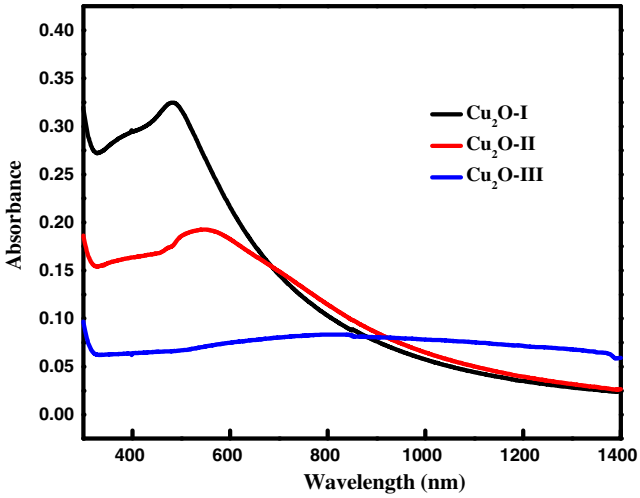

Figure 2. UV–Vis absorption spectrum of the as-synthesized Cu_2O powders at different NaOH concentrations.

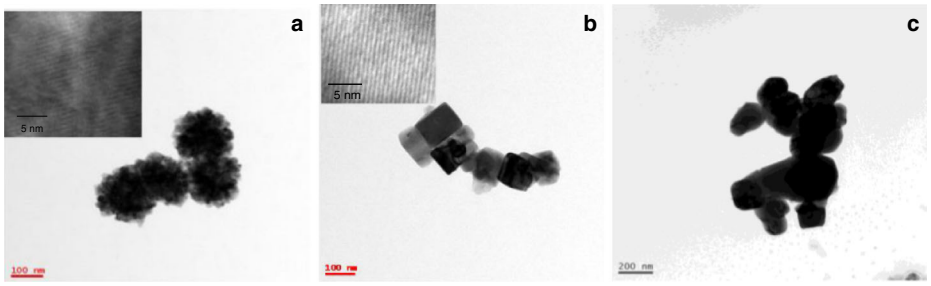

Figure 3. TEM images of (**a**) Cu_2O-I, (**b**) Cu_2O-II and (**c**) Cu_2O-III.

Former studies on Cu_2O were done at nano- and femtosecond regimes [3,10,11]. The present studies focus on the optical nonlinearities of cuprous oxide at picosecond regime. Second harmonic from the Nd:YAG laser with 30 ps (EKSPLA-PL2143-SH) pulse duration and 10 Hz repetition rate was used as the excitation sources for nonlinear absorption (NLA) measurements in the ps regime. Figure 4 shows intensity-dependent open-aperture Z-scan traces of Cu_2O powder (1.3×10^{-3} M) in isopropanol. The nonlinear optical response of the pure solvent (isopropanol) was first recorded in the range of intensities used with the 532 nm excitation wavelength and we observed no nonlinear response. Also, the linear absorption coefficient of the samples was measured by the conventional method on the basis of $\alpha_0 = -(1/L)\ln(T_0)$ is the low intensity (linear regime) absorption coefficient.

For Cu_2O system, we see that the valley in the Z-scan trace increases monotonically with increase in intensity due to strong ESA as well as two-photon absorption (TPA). Therefore, as both ESA and TPA contribute to the RSA behaviour observed and as it is very difficult to separate their contributions, β_{eff} combines both ESA and TPA contributions towards the RSA behaviour. In this case, optical intensity variation of the laser beam propagating through a thin nonlinear absorber is governed by the differential equation

$$\frac{\mathrm{d}I}{\mathrm{d}z} = -\alpha(I)I, \tag{1}$$

where $\alpha(I)$ is the total nonlinear absorption coefficient and z is the propagation distance in the medium. To analyse this type of switchover from SA to RSA, the observed

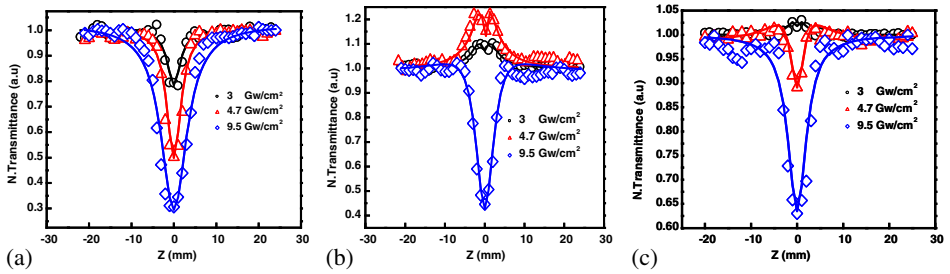

Figure 4. Intensity-dependent open-aperture Z-scan curves of (**a**) Cu_2O-I, (**b**) Cu_2O-II and (**c**) Cu_2O-III at picosecond regime (open circles, open triangles and open squares are experimental curves and solid lines are the theoretically generated curves).

experimental data are fitted with the following equation that combines the saturation behaviour with saturation intensity I_s and the effective excited state absorption coefficients (β_{eff}) that included both the ESA and TPA.

$$\alpha(I) = \frac{\alpha_0}{1 + (I/I_s)} + \beta_{eff} I, \tag{2}$$

where the first term describes the saturation and the second term describes RSA including possible ESA and TPA. α_0 is the linear absorption coefficient at 532 nm. I and I_s represent the laser intensity at each position of the Z-scan and saturation intensity of the sample respectively. In figure 4 solid lines show theoretical fit to the experimental data using the above equations, where I_s and β_{eff} have been used as fitting parameters to match the peak and valley, in the experimental data. The normalized transmittance at $z = 0$ of the Cu_2O-I nanoclusters is ~ 0.29, Cu_2O-II microcubes is ~ 0.42 and Cu_2O-III microparticles is ~ 0.63 for an input intensity of 9.5 GW cm^{-2}. At 3 GW cm^{-2} peak intensity, for Cu_2O-I the calculated β_{eff} is 6.19×10^{-10} cm W^{-1}. For Cu_2O-II and Cu_2O-III, the estimated values of I_s and β_{eff} are 1×10^9, 2.5×10^9 W cm^{-2} and 3.28×10^{-10}, 1×10^{-10} cm W^{-1} respectively. In this paper, we present the nonlinear absorption measurement of Cu_2O with different morphologies. Effective nonlinear absorption coeiffient (β_{eff}) values for nanoclusters are higher compared to the microcubes and microparticles due to quantum size effects.

Acknowledgement

DNR acknowledges the DST financial support through the ITPAR phase-III project.

References

[1] H Sekhar and D Narayana Rao, *J. Mater. Sci.* **47**, 1964 (2012)
[2] H Sekhar and D Narayana Rao, *J. Alloys Compounds* **517**, 103 (2012)
[3] H Sekhar and D Narayana Rao, *J. Nanopart. Res.* **14**, 976 (2012)
[4] M Sheik-Bahae, A A Said, T Wei, D J Hagan and E W Van Stryland, *IEEE J. Quantum Electron.* **26**(**4**), 760 (1990)
[5] P Prem Kiran, S Venugopal Rao, M Ferrari, B M Krishna, H Sekhar, S Alee and D Narayana Rao, *Nonlin. Opt. Quantum Opt.* **40**, 223 (2010)
[6] H Sekhar, P Prem Kiran and D Narayana Rao, *Mater. Chem. Phys.* **130**, 113 (2011)
[7] H Sekhar, P Prem Kiran and D Narayana Rao, *Proc. SPIE* **7712**, 77122J (2010)
[8] Q Li, C Liu, Q Gong, J Gao and L Qi, *J. Nanopart. Res.* **11**, 989 (2009)
[9] X Zhang, J Song, J Jiao and X Mei, *Solid State Sci.* **12**, 1215 (2010)
[10] Q Li, C Liu, Q Gong, J Gao and L Qi, *J. Nanopart. Res.* **11**, 989 (2009)
[11] M Fu, H Long, K Wang, G Yang and P Lu, *Thin Solid Films* **519**, 6557 (2011)